Available online at www.sciencedirect.com

ScienceDirect

Procedia CIRP 133 (2025) 364–369

www.elsevier.com/locate/procedia

20th CIRP Conference on Modeling of Machining Operations

Rheological properties and machinability in dry turning of neat PLA and PLA reinforced with hemp fibers

Liam Cloëz[a,b,*], Michaël Fontaine[a], Thierry Barrière[b], Alexandre Gilbin[a]

Applied Mechanics Dept., FEMTO-ST Institute, UMR CNRS 6174, UFC/ENSMM, 24 rue de l'Epitaphe, F-25000 Besançon, France
[a] SUPMICROTECH-ENSMM, [b] Université de Franche-Comté

* Corresponding author. Tel.: +33611190675. *E-mail address:* liam.cloez@femto-st.fr

Abstract

Society still overuses polymers without fully considering their environmental impact. However, attention is increasingly shifting towards biocomposites, which already have practical applications in various fields. Despite progress, finding alternatives for complex, precise parts remain challenging. This is why we are focusing on hybrid manufacturing, which combines the benefits of 3D printing and machining. 3D printing allows us to produce parts with complex geometries, while machining ensures the precision required to meet the highest technical standards. However, this combination of processes can present challenges. Lubricants cannot be used in cutting to prevent affecting the printed layers and hydrophilic fibers. Without lubrication, localized heating occurs during machining, and since polymers are thermally insulating, this can cause material melting, degrading the surface and quality of the part. Therefore, it is essential to first study the dry machinability of these materials to prevent such issues. This study is part of a broader approach aimed at exploring the combination of Pellets Additive Manufacturing (PAM) and milling, particularly on a biocomposite composed of 80% PLA and 20% hemp fibers. However, this aspect is not directly addressed here. Instead, this paper focuses on understanding the cutting behavior of PLA, both pure and reinforced, by analyzing the influence of cutting parameters through turning operations on injection-molded parts. The objective is to assess their impact on surface integrity and cutting forces. This approach facilitates the study of fundamental cutting parameters. Optimal cutting parameters for these materials are identified by analyzing cutting forces and assessing surface quality.

Keywords: Poly Lactic Acid ; Natural fibers ; Dry machining ; Turning ; Injection molding

1. Introduction

Composites have become integral to various industries, profoundly influencing modern life. Despite their advantages in versatility and durability, the environmental impact of their widespread use cannot be ignored. Traditional polymers heavily rely on non-renewable petrochemical resources, contributing to greenhouse gas emissions and environmental degradation. This challenge has prompted a growing interest in sustainable alternatives to address the ecological concerns associated with polymers. Biocomposites have already been studied for various applications, including medical applications [1], civil construction [2] and transport applications. Biosourced polymers, or "bioplastics," are gaining recognition as a viable solution. Studies have been conducted to compare the ecological impact of a bioplastic and a synthetic polymer. Belboom et al.[3], for example, studied the biobased HDPE in comparison to its fossil counterpart. The ecological impact of the biobased polymer is reduced in terms of CO2 emissions compared to the fossil one. However, other impact categories still require improvements, especially those related to the cultivation and transformation stages of raw materials.

10.1016/j.procir.2025.02.063

Polylactic acid (PLA) is a leading bioplastic, valued for its biodegradability and favorable mechanical properties. When reinforced with natural fibers such as hemp, PLA composites exhibit improved stiffness, tensile strength, and thermal stability, making them suitable for applications in packaging, automotive components, and 3D printing [4]. However, as Schäfer et al. [5] emphasize, assessing the recyclability and life-cycle performance of such composites is essential to ensuring their long-term sustainability. Despite its potential, the machining of hemp-reinforced PLA composites remains underexplored. Injection molding is a well-established process for fabricating complex components at scale, but machining operations, such as milling or drilling, may cause issues such as thermal effects, formation of burrs, delamination or tool wear [6]. Rawal et al. [6] highlights factors that influence composite machining, including machining conditions, tool selection, fabrication method and composite composition. In the case of hemp-reinforced PLA, the interactions between the fibers and the PLA matrix affect mechanical and thermal behaviors, introducing additional complexity. To overcome these challenges, it is crucial to conduct detailed characterizations of the thermal, mechanical, and rheological properties of hemp-reinforced PLA composites. Such analyses provide insights into the material's performance under various conditions, enabling the optimization of injection molding parameters and machining techniques. By understanding these behaviors, manufacturers can produce high-quality components while preserving the environmental benefits of this sustainable composite, positioning it as a promising material for future applications.

2. Materials and methods

2.1. Materials

The materials used for this study are poly (lactic acid) PLA and hemp fiber-reinforced PLA. The first is provided by the company NaturePlast under the reference PLI005 [7]. The second material consists in a composite made of a PLA matrix from Total Corbion (reference Luminy L175 [8]) loaded with 20 wt.% of hemp fibers. In both materials of the study, the PLA has a D-lactide content below 1%, a density of 1.24 g.cm^{-3}, a melting point (T_m) in the range of 170–180 °C, and a glass transition temperature (T_g) near 60 °C. For the rest of the study, the first material will be named PLI005, and the second will be named L175-H20. Materials are provided in pellet form, requiring careful drying before processing. While the supplier advises drying at 60 °C for 3 hours for PLI005 and at 100 °C for 4 hours at 6 hours for L175-H20, experimental investigations in our laboratory have been made to ensure this point. We identified that drying at 80 °C for PLI005 and at 100 °C for L175-H20 for a minimum of 5 hours was effective in reducing the impact of residual moisture, ensuring better thermal stability and minimizing degradation during processing. Prior to testing or characterization, samples are conditioned for a minimum of 14 days in a controlled environment at 23 °C and 50% relative humidity (RH).

2.2. Differential Scanning Calorimetry (DSC)

Thermal behavior of the material was analyzed using a SETARAM DSC131EVO differential scanning calorimeter. The study focused on identifying key thermal transitions, including melting temperature (T_m), crystallization temperature (T_c), and glass transition temperature (T_g). Samples of PLA pellets, weighing 27.3 mg, were placed in aluminum crucibles and subjected to a heating rate of 3 °C.min^{-1}, starting at 25 °C and gradually increasing to 300 °C. Once the maximum temperature was reached, the material was cooled back to 25 °C under ambient air. This procedure provided detailed insights into the thermal stability and phase transitions of the PLA matrix under elevated temperatures.

2.3. Rheometers

The rheological properties of the material were evaluated using two different rheometers. The first instrument, a HAAKE MARS equipped with a cone-and-plate system, was employed to measure the shear viscosity of the polymer under varying shear rates, ranging from 10^{-5} s^{-1} to 10^2 s^{-1}, at multiple temperatures. The sample was placed on a plate with a diameter of 35 mm, while the cone, featuring an air gap angle (β) of 2°, was positioned above. During the test, the cone was rotated at a defined angular velocity (ω) as the sample was heated to the desired temperature. The second instrument used for rheological analysis was a ROSAND RH2000 capillary rheometer. In this setup, the polymer was extruded through a capillary die with a diameter of 1 mm and a length of 16 mm. Pressure sensors positioned at the inlet and outlet of the die allowed for precise determination of the material's shear viscosity. This system is particularly suited for evaluating polymer viscosity at elevated shear rates, ranging from 10^2 s^{-1} to 10^4 s^{-1}.

2.4. Tensile test machine

Tensile strength, elongation at break, and Young's modulus were determined on PLA and reinforced PLA specimens prepared via injection molding, in accordance with the ISO 527-2 standard [9]. There are 4 samples tested per material. The tensile tests were carried out using an MTS C45 testing machine, equipped with a 5 kN load cell. The tests were performed at a crosshead speed of 2 mm.min^{-1}.

Table 1. Injection molding parameters for both materials

Material	PLI005	L175-H20
Feed zone [°C]	220	200
Transition zone [°C]	215	195
Metering zone [°C]	210	190
Mold temperature [°C]	25	25
Injection flow [g.s^{-1}]	41	35
Injection pressure [MPa]	14	12
Cooling time [s]	25	25

2.5. Injection molding

The injection molding was carried out using a BOY 22M with a clamping force of 220 kN. The materials were introduced into the injection molding press in pellet form and injected to tensile test specimen or turning cylinders. The injection molding parameters are outlined in Table 1.

2.6. Machining

Dry turning tests were conducted on a 4-axis DOOSAN Lynx 220Y to study the machinability of pure PLA and PLA reinforced with hemp fibers. The specimen dimensions are detailed in Figure 1. To address the specific challenges of dry machining these materials, a longitudinal turning operation was selected as the primary machining process. The cutting tool used is a CCGT 09T304-FN2-WNN10 insert from Walter Tools, which is mounted on the KISTLER 9129AA dynamometer to accurately measure cutting forces. Data acquisition is carried out at a fixed sampling frequency of 1000 Hz to facilitate handling between each test while ensuring a minimum of 10 measured points per revolution for the highest cutting speeds. This choice is perfectly acceptable for continuous cutting and ensure consistent and reliable measurement resolution throughout the tests. Only one cutting tool was used during these machining tests, and it did not showed sign of wear according to the ISO 3685 standard [10].

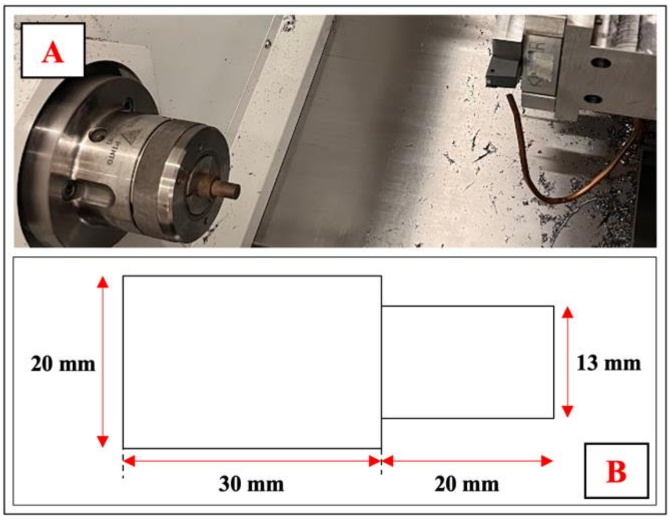

Figure 1: Picture of the experiment with the cutting tool fixed on the Kistler sensor (A) and the geometry of the cylinder with the machined area hatched (B)

2.7. Optical 3D measuring instrument

The optical coordinate measuring machine µCMM from Bruker Alicona, was used to evaluate the arithmetic average roughness (*Ra*) of the machined parts. Measurements were performed over an 8 × 1 mm area, centered within the groove and aligned with the feed direction. The data were analyzed using Digital Surf Mountains Map software. According to the ISO 21920 standard [11], the cut-off was selected to be 0.8 mm and the evaluation lengths are 8 mm, although the standard specifies a minimum evaluation length of 4 mm. Each roughness profile measurement is repeated 5 times.

3. Results and discussion

3.1. Thermal properties

In Figure 2, the DSC thermogram displays two curves: the blue curve represents pure PLA, while the red curve corresponds to the biocomposite. The first endothermic phase transition corresponds to the glass transition (T_g) at 58 °C for PLA and supposed to be 60 °C for the matrix of the composite according to the Total-Corbion company [8]. Next, the second phase transition is exothermic and corresponds to the crystallization of the material (T_c) at 106 °C for PLA and 112 °C for the biocomposite. Finally, the last endothermic phase transition corresponds to the melting temperature (T_m), which is approximately 174 °C for PLA and 179 °C for the biocomposite. The melting temperature given by Total-Corbion for the PLA from the biocomposite (L175) is 175 °C.

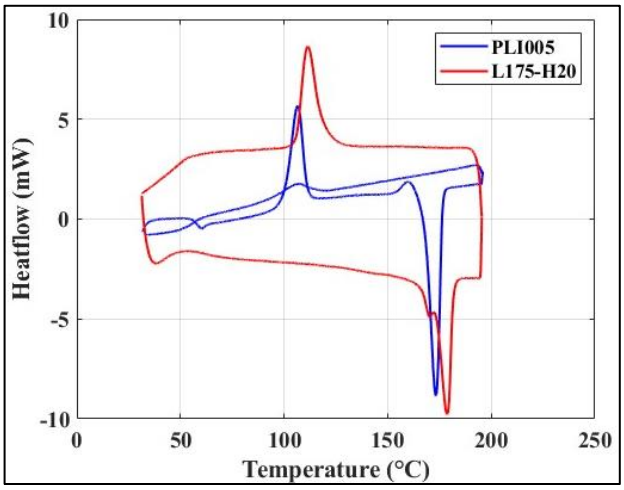

Figure 2 : DSC thermograms of PLA (blue) and L175-H20 (red)

The addition of hemp fibers affects the thermal properties and crystallinity of PLA-based composites. N.F. Niang studied this influence on the same PLA (PLI005) reinforced with hemp fibers [12]. The relative stability of the glass transition temperature and the melting temperature indicates that the material's thermal stability is preserved with hemp fiber reinforcement. However, the broadened melting intervals and slightly increased crystallization temperatures suggest interactions between the PLA matrix and hemp fibers. Moreover, the degree of crystallinity rises as the fiber content increases [12], [13], highlighting the role of hemp fibers in promoting nucleation and enhancing crystal growth. This behavior underlines the influence of reinforcement on the structural organization of the material.

3.2. Rheological properties

In Figure 3, the shear viscosity profiles reveal pseudoplastic behavior. A Newtonian plateau is observed at low shear rates (up to 1 s^{-1}), followed by a decrease in viscosity as the shear rate increases, confirming the shear-thinning nature of PLA.
Viscosity also reduces with increasing temperature, demonstrating the thermo-sensitive response of the material. These patterns are consistent with previous findings on PLA

rheology. For example, Lacambra-Andreu et al. [14] reported similar trends but with higher viscosity values. The addition of hemp fibers significantly affects the viscosity of the composite. The fibers increase the viscosity due to their reinforcing effect on the PLA matrix. This increase results from interactions between the matrix and the fibers, which enhances the structural integrity of the composite material. Furthermore, this reinforcing effect is supported by improvements in the tensile and flexural moduli, as reported in studies such as Sawpan et al. [15].

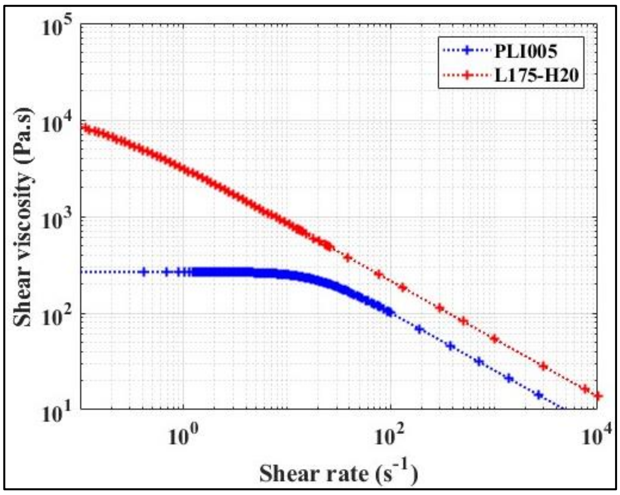

Figure 3 : Shear viscosity depending on shear rate for PLA and PLA-H20 at 200 °C

3.3. Mechanical properties

Figure 4 presents the mechanical properties of injected PLA and PLA reinforced with hemp fibers, as tested under the parameters outlined in Table 1. To measure longitudinal deformation, an MTS axial extensometer was affixed to the effective section of the specimens. The stress-strain curves demonstrate a brittle material behavior, with the samples breaking abruptly without displaying necking. Sawpan conducted a comprehensive mechanical characterization of PLA and hemp fiber-reinforced PLA under various loading conditions, including flexion, impact, and tensile tests [15].

For tensile properties, a similar trend was observed: the maximum stress increased with higher reinforcement content, while the strain at break decreased as fibers were added. The Young's modulus of the reinforced PLA nearly doubled compared to that of pure PLA, consistent with Sawpan's findings. It is observed that adding hemp fibers increases the dispersion of the measurements due to the heterogeneity they introduce.

3.4. Machinability

To overcome the technical challenges associated with machining PLA and fiber-reinforced PLA under dry conditions, tests were conducted in accordance with the NF E66-520 standard [16] to study the tool-workpiece interaction. The experiments were repeated three times to ensure repeatability. Each measurement corresponds to a machining pass, with a pause between measurements. Given that the cutting occurs in an unconstrained environment, with machining times ranging from 1 to 20 seconds, the heating did not affect the cutting of the workpiece within the studied cutting parameters. Additionally, no material tearing was observed. However, such phenomena are observed during dry milling operations [17]. To evaluate the machinability of the material, various tests were performed to determine the cutting parameters. These parameters were analyzed using the specific cutting coefficient (K_c), chip formation, and surface roughness of the machined parts while varying the cutting speed (V_c) and feed rate per revolution (*f*). The specific cutting coefficient can be determined by equation 1 [16], where F_c is the cutting force and a_p the depth of cut in turning. The calculation of K_c is essential to identify the minimum cutting speed where K_c starts to stabilize and to detect phenomena specific to the cutting speed.

$$K_c = \frac{F_c}{f \cdot a_p} \quad (1)$$

In Figure 5A, the specific cutting coefficient is analyzed as a function of cutting speed, with the feed per revolution *f* and depth of cut a_p fixed at 0.15 mm/rev and 1 mm, respectively. These parameters were selected as reference values based on preliminary tests. The cutting speed ranges from 20 m/min to 250 m/min, limited by the workpiece diameter and machine capabilities. For pure PLA, the coefficient decreases with increasing cutting speed, a trend that is less pronounced for reinforced PLA. At 150 m/min, a sudden peak is observed for the reinforced PLA, suggesting the need for further testing to confirm these measurements.

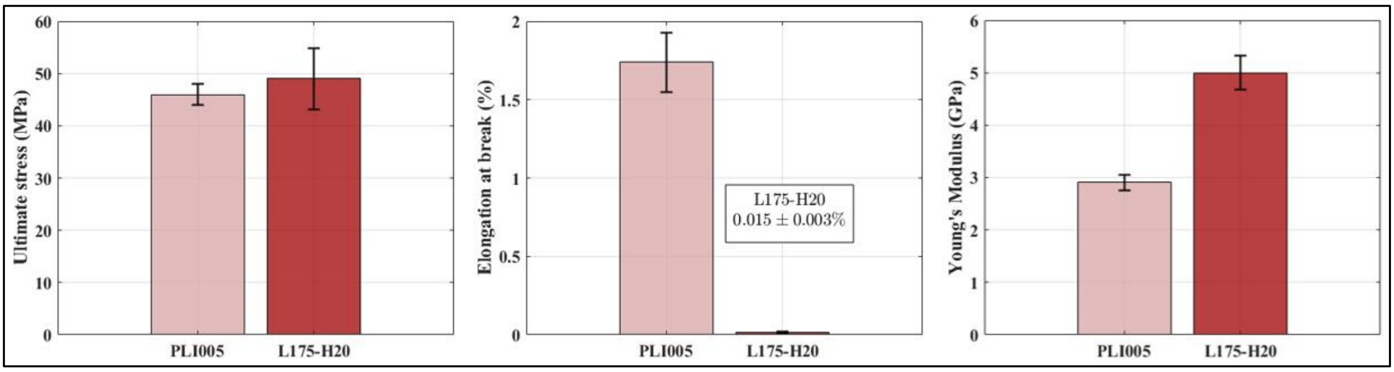

Figure 4 : Tensile mechanical properties of PLI005 and L175-H20

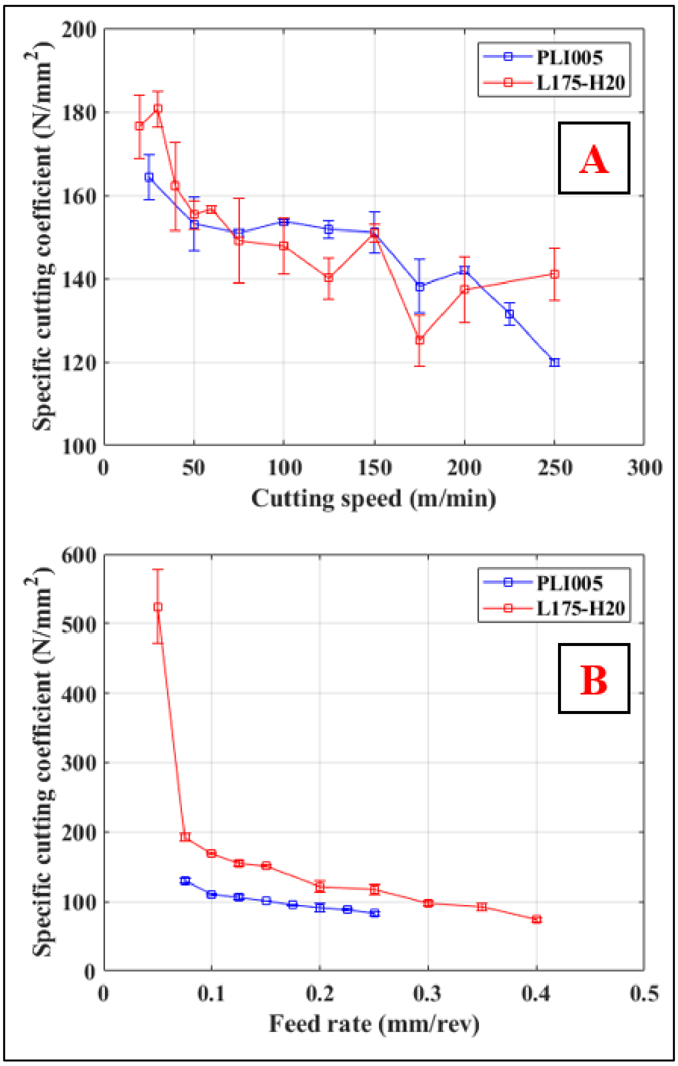

Figure 5 : Effect of cutting speed (a_p = 1 mm, f = 0.15 mm/rev) on the average specific cutting coefficient on PLI005 and on L175-H20 (A). Effect of feed rate on the average specific cutting coefficient on PLI005 (a_p = 1 mm, V_c = 75 m/min) and on L175-H20 (a_p = 1 mm, V_c = 150 m/min) (B).

In Figure 6A, the arithmetic average roughness varies minimally with cutting speed, indicating that cutting speed does not significantly affect roughness. Consequently, it does not provide the necessary insights to determine the minimum cutting speed in this context. Chip morphology appears as entangled ribbon-like chips [16] across all cutting speeds studied. Based on these initial tests, minimum cutting speeds were selected for subsequent experiments, which focus on varying feed rates while keeping the cutting speed constant at 150 m/min for L175-H20 and 75 m/min for PLI005. For PLI005, a cutting speed of 75 m/min allows for better repeatability, and for L175-H20, the created surface shows no visible defects caused by machining. In Figure 5B, the cutting coefficient is examined as a function of feed per revolution, with the depth of cut kept constant and the cutting speed fixed at its minimum. The feed per revolution ranges from 0.075 mm/rev to 0.25 mm/rev for PLI005 and from 0.05 mm/rev to 0.4 mm/rev for L175-H20. The range of feed rates tested for the PLI005 is reduced compared to the L175-H20 due to a very poor cut. The results show similar trends, with K_c decreasing as feed per revolution increases. However, unlike the previous tests where K_c values were relatively close, here the values are doubled or even quadrupled for lower feed rates. As feed per revolution increases, the K_c values converge. The figure 6B reveal significant variations in surface roughness. The roughness is very high at low feed rates, decreases to a minimum due to the chip wrapping around the workpiece. It then decreases to a minimum before rising again at higher feed rates, where vibrational phenomena occur, causing repeated material removal and affecting surface quality. The theoretical Ra aligns well with the measured curves, however, the observed discrepancies can be attributed to physical processes not considered in the model, such as fiber pull-out, thermal effects of the fiber-reinforced PLA, or tool wear and vibrations. To improve the theoretical model, it would be beneficial to integrate the properties of the fibers and matrix, as well as thermal and dynamic phenomena, to better reflect actual machining conditions and reduce these discrepancies. The theoretical Ra (µm) can be determined by the equation 2 adapted from [18], where R_ε is the tool nose radius and is 0.8 mm.

$$Ra = \frac{f^2}{18\sqrt{3}\times R_\varepsilon} \quad (2)$$

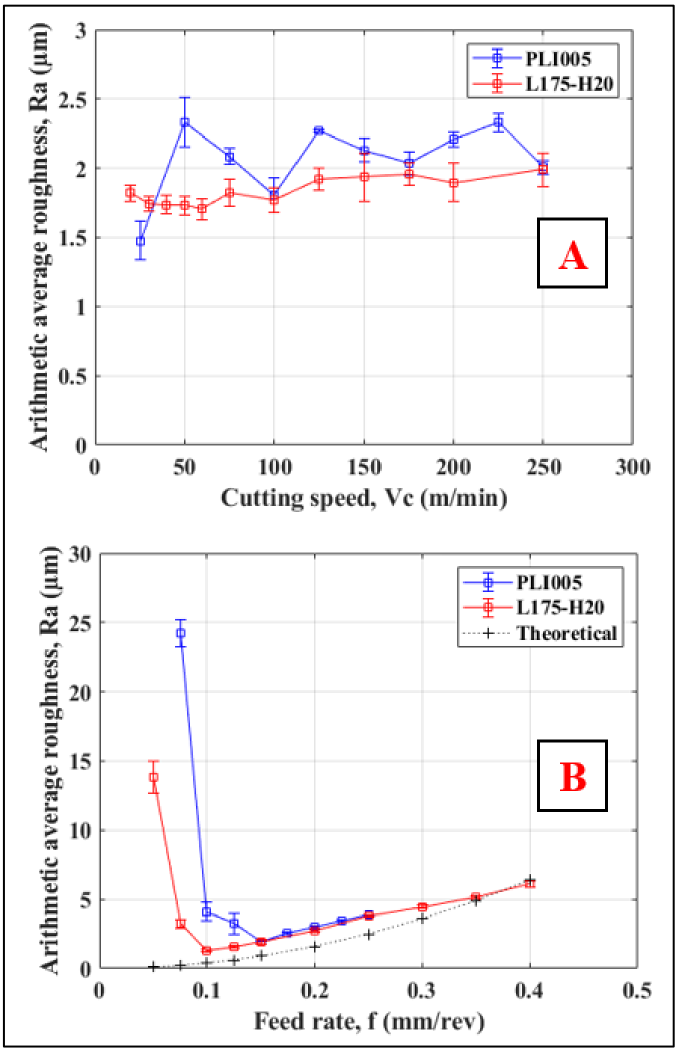

Figure 6 : Effect of cutting speed (a_p = 1 mm, f = 0.15 mm/rev) on the arithmetic average roughness on PLI005 and on L175-H20 (A). Effect of feed rate on the arithmetic average roughness on PLI005 (a_p = 1 mm, V_c = 75 m/min) and on L175-H20 (a_p = 1 mm, Vc = 150 m/min) (B).

Through chip formation, observable changes can be identified. For small feed rates ranging from 0.05 mm/rev to 0.15 mm/rev, entangled ribbon-like chips are observed. For feed rates between 0.2 mm/rev and 0.25 mm/rev, attached arc-shaped chips are formed. Finally, for feed rates from 0.3 mm/rev to 0.4 mm/rev, detached arc-shaped chips [16] are produced. Based on this data, it is possible to select an appropriate range of feed rates for the given material and tool combination.

4. Conclusion and prospects

This paper presents preliminary results on the turning of neat PLA and PLA reinforced with hemp fibers, under dry machining conditions. These conditions were chosen to replicate those used for hybridization, enabling a consistent comparison of machining performance. First, these results allow for the selection of suitable parameters for injection molding (Table 1). Moreover, various tests, including thermal, mechanical, and rheological analyses, were conducted, and their results are consistent with those reported in the literature. Secondly, we have a better comprehension of the machinability of these materials. For both reinforced and unreinforced PLA, a similar decreasing trend of K_c is observed, whether as a function of cutting speed or feed rate. For PLI005, the minimum cutting speed was selected at 75 m/min. In the case of L175-H20, a rise in K_c is observed at 150 m/min, necessitating further tests to validate these results using additional injection-molded cylinders. Consequently, tests varying the feed rate were conducted at a cutting speed of 150 m/min. The optimal feed rate range for PLI005 lies between 0.15 and 0.175 mm/rev. At lower feed rates, the chip wraps around the workpiece, leading to surface defects or irregularities. At higher feed rates, vibrational phenomena occur, causing repeated material removal and impacting surface quality. For L175-H20, the optimal feed rate range appears to be broader, between 0.1 and 0.2 mm/rev. At lower feed rates, the same phenomena are observed as with PLI005, including chip wrapping around the workpiece, which affects surface quality. At higher feed rates, machining marks become clearly visible, resulting in a less desirable surface finish. The thermal aspect was not addressed in the cutting tests and will be necessary to correlate the machinability of the material with its thermal behavior. As stated by Dilberoglu et al. [19], exceeding the glass transition temperature can lead to a decrease in surface quality. Depperman et al. [20] studied this correlation using the Peclet number to determine the thermal transfer phenomena during dry machining of a metal and limit the accumulation of heat in the cutting zone. More detailed analyses, such as fiber pull-out and its impact on the final surface finish, were not addressed in this paper but will be the focus of a future study. Although this study provides valuable insights into the machining behavior of PLA and reinforced PLA, a specific experimental validation on PAM-printed parts is necessary to ensure the transferability of the results to a hybrid process combining additive manufacturing and milling.

Acknowledgements

The authors gratefully acknowledged the financial support received from the French Ministry of Higher education and scientific research. Experimental tests were carried out thanks to SupMicroTech-ENSMM workshop and MIFHYSTO platform for rheology, injection molding, cutting forces measurement and metrology. This work was carried out within the Manufacturing 21 network, which gathers about 20 French research laboratories. The covered topics are the study and modelling of the manufacturing processes, especially machining and additive manufacturing, and the emergence of new manufacturing methods.

References

[1] S. Ramakrishna, J. Mayer, E. Wintermantel, and K. W. Leong, "Biomedical applications of polymer-composite materials: a review," *Composites Science and Technology*, vol. 61, no. 9, pp. 1189–1224, 2001, doi: 10.1016/S0266-3538(00)00241-4.

[2] E. Bodros, I. Pillin, N. Montrelay, and C. Baley, "Could biopolymers reinforced by randomly scattered flax fibre be used in structural applications?," *Composites Science and Technology*, vol. 67, no. 3–4, pp. 462–470, 2007, doi: 10.1016/j.compscitech.2006.08.024.

[3] S. Belboom and A. Léonard, "Does biobased polymer achieve better environmental impacts than fossil polymer? Comparison of fossil HDPE and biobased HDPE produced from sugar beet and wheat," *Biomass and Bioenergy*, vol. 85, pp. 159–167, 2016, doi: 10.1016/j.biombioe.2015.12.014.

[4] V. K. Balla, K. H. Kate, J. Satyavolu, P. Singh, and J. G. D. Tadimeti, "Additive manufacturing of natural fiber reinforced polymer composites: Processing and prospects," *Composites Part B: Engineering*, vol. 174, p. 106956, Oct. 2019, doi: 10.1016/j.compositesb.2019.106956.

[5] H. Schäfer, C. Pretschuh, and O. Brüggemann, "Reduction of cycle times in injection molding of PLA through bio-based nucleating agents," *European Polymer Journal*, vol. 115, pp. 6–11, 2019, doi: 10.1016/j.eurpolymj.2019.03.011.

[6] J. Babu, T. Sunny, N. A. Paul, K. P. Mohan, J. Philip, and J. P. Davim, "Assessment of delamination in composite materials: A review," *Proceedings of the Institution of Mechanical Engineers, Part B: Journal of Engineering Manufacture*, vol. 230, no. 11, pp. 1990–2003, 2016, doi: 10.1177/0954405415619343.

[7] NaturePlast, "NaturePlast®PLI005TechnicalDataSheet," 2017.

[8] Total Corbion PLA, "Luminy®L175ProductDataSheet," 2019.

[9] ISO, *Plastics - Determination of tensile properties - Part 2: Test conditions for moulding and extrusion plastics*, ISO 527-2, 2012.

[10] ISO, *Tool life testing with a single cutting edge*, ISO 3685, 1993.

[11] ISO, *Geometrical product specifications (GPS) - Surface texture: Profile - Part 3: Height parameters*, ISO 21920-3, 2021.

[12] N. F. Niang, T. Barrière, V. Placet, and S. Holopainen, "Optimisation de la fabrication additive de composites biosourcés renforcés par des fibres courtes de chanvre," in *JNC23: Journées Nationales sur les Composites 2023*, 2023. [Online]. Available: hal-04606807

[13] L. Aliotta, V. Gigante, M.-B. Coltelli, P. Cinelli, A. Lazzeri, and M. Seggiani, "Thermo-Mechanical Properties of PLA/Short Flax Fiber Biocomposites," *Applied Sciences*, vol. 9, no. 18, 2019, doi: 10.3390/app9183797.

[14] X. Lacambra-Andreu, X. P. Morelle, A. Maazouz, J.-M. Chenal, and K. Lamnawar, "Rheological investigation and modeling of healing properties during extrusion-based 3D printing of poly(lactic-acid)," *Rheol Acta*, vol. 62, no. 1, pp. 31–44, 2023, doi: 10.1007/s00397-022-01377-6.

[15] M. A. Sawpan, K. L. Pickering, and A. Fernyhough, "Characterisation of hemp fibre reinforced Poly(Lactic Acid) composites," *IJMPT*, vol. 36, no. 1/2/3/4, p. 229, 2009, doi: 10.1504/IJMPT.2009.027834.

[16] AFNOR, *Cutting tool performance - Tool-material pair - Part 3: Application to turning technology*, NF E66-520-3, France., 1997.

[17] L. Cloëz, "Machinability of PLA obtained by injection molding under a dry milling process," presented at the Material Forming, Materials Research Proceedings, May 2024, pp. 1877–1886. doi: 10.21741/9781644903131-208.

[18] S. Vajpayee, "Analytical study of surface roughness in turning," *Wear*, vol. 70, no. 2, pp. 165–175, 1981, doi: 10.1016/0043-1648(81)90151-4.

[19] U. M. Dilberoglu, U. Yaman, and M. Dolen, "A comprehensive guide to milling techniques for smoothing the surfaces of 3D-printed thermoplastic parts," *Rapid Prototyping Journal*, vol. 38, no. 8, pp. 1648–1662, doi: 10.1108/RPJ-08-2023-0277.

[20] M. Deppermann and R. Kneer, "Determination of the heat flux to the workpiece during dry turning by inverse methods," *Prod. Eng. Res. Devel.*, vol. 9, no. 4, pp. 465–471, Oct. 2015, doi: 10.1007/s11740-015-0635-6.